magnetochemistry

MDPI

Article

A New Family of High T_c Molecule-Based Magnetic Networks: V[x-Cl_nPTCE]$_2$·yCH_2Cl_2 (PTCE = Phenyltricyanoethylene)

David S. Tatum, Joseph M. Zadrozny and Gordon T. Yee *

Department of Chemistry, Virginia Tech, Blacksburg, VA 24061, USA

* Correspondence: gyee@vt.edu (G.T.Y.); dtatum@lumiphore.com (D.S.T.); Joe.Zadrozny@colostate.edu (J.M.Z.)

Received: 25 June 2019; Accepted: 19 July 2019; Published: 1 August 2019

Abstract: Using the structural and electronic tunability of molecules to control magnetism is a central challenge of inorganic chemistry. Herein, a ten-member family of the high-ordering temperature (T_c) molecule-based magnetic coordination networks of the form V[x-Cl_nPTCE]$_2$·yCH_2Cl_2 (PTCE = phenyltricyanoethylene, $y < 0.5$) were synthesized and characterized, where x is (are) the position(s) and n is the number of chlorine substitutions on the phenyl ring. These chlorophenyltricyanoethelenes are tunable analogs of the more commonly investigated tetracyanoethylene (TCNE). Varying the number and position of chlorine substitution around the phenyl ring engendered a family of network solids with significantly different magnetic ordering temperatures ranging from 146 to 285 K. The T_cs of these ferrimagnets were rationalized with the aid of cyclic voltammetry and Density Functional Theory (DFT) calculations.

Keywords: molecule-based ferrimagnetism

1. Introduction

The ferrimagnet V[TCNE]$_2$·yCH_2Cl_2 (where $y < 0.5$) was discovered in 1991, and improved syntheses have yielded samples with ordering temperatures (or critical temperatures, T_cs) up to 400 K [1–3]. As a room temperature magnetic semiconductor, films of V[TCNE]$_2$ show potential for application in spintronics [4,5], a point emphasized by the extremely narrow ferromagnetic resonance spectra [6]. Efforts by us and others to tune the properties of V[TCNE]$_2$-like magnets have involved the preparation of compounds with other transition metal ions [7], combinations of metal ions [8,9], and other conjugated polynitriles [10–17]. Recently, we reported a family of tunable fluorophenyltricyanoethylene-based magnets, V[x-F_nPTCE]$_2$, which ranged in T_c from 160 to 315 K [18–20]. The T_cs of the V[x-F_nPTCE]$_2$ networks displayed a significant dependence on the position of the fluorine substitution, and the trend was rationalized using a combination of steric and electronic effects based on electrochemical and computational data. Comprehensive and systematic magnetochemical studies of this kind offer insight into the factors that govern magnetic ordering within V[TCNE]$_2$-like magnets, with the aim of eventually exploiting these factors to develop improved, higher-T_c materials. Herein, we extend these substituent-effect studies to analogous magnets of the form V[x-Cl_nPTCE]$_2$. In particular, we were interested in the larger size of Cl relative to F, since we previously demonstrated that the larger size of F relative to H enhanced T_c by increasing the dihedral angle between the phenyl ring and olefin [18]. We were also interested in investigating the change in electronegativity between F and Cl to compare the impacts on T_c by the positional electronic effects of each halogen substitution. In order to facilitate these comparisons, ten new chlorophenyltricyanoethylene one-electron acceptors (Figure 1) were synthesized, the magnetic

properties of the corresponding V[x-Cl_nPTCE]$_2$ magnets were characterized, and the results were rationalized with the aid of measured and calculated acceptor properties.

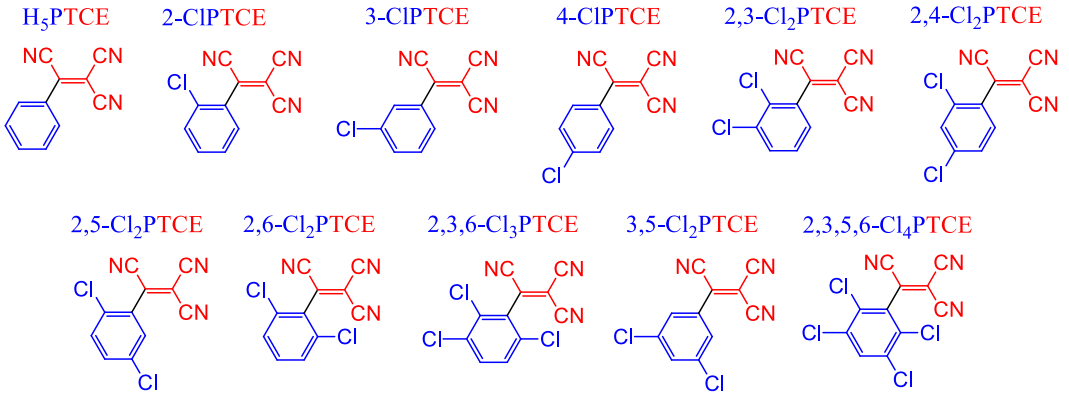

Figure 1. Structures and names of the chlorine substituted (and unsubstituted parent) PTCE one-electron acceptors.

2. Results

The chlorophenyltricyanoethylene acceptors were synthesized in moderate yield starting from the appropriately substituted chlorobenzaldehydes (Scheme 1). Most benzaldehydes were available commercially, while others were synthesized in one step from commercially available substituted benzenes (Supplementary Materials).

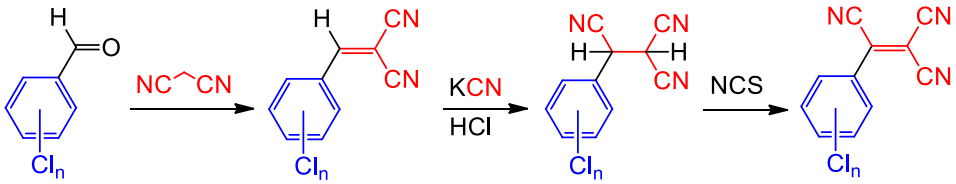

Scheme 1. Synthesis of organic one-electron acceptors (NCS = N-chlorosuccinimide).

The reaction of two equivalents of a given acceptor with vanadium hexacarbonyl yields a black, insoluble solid, which is collected upon solvent removal as a free-flowing powder (Scheme 2) [1–3]. Elemental analysis indicates a 2:1 acceptor:vanadium ratio in the isolated product with less than 0.5 equivalents of residual CH_2Cl_2 in all cases, which is consistent with the stoichiometry and residual solvent observed for analogous magnets of this type. For the sake of simplicity, residual solvent will not be included in subsequent formulas.

$$V(CO)_6 + 2[x\text{-}Cl_nPTCE] \xrightarrow{CH_2Cl_2} V[x\text{-}Cl_nPTCE]_2 \cdot yCH_2Cl_2 + 6CO$$

Scheme 2. Preparation of V[x-Cl_nPTCE]$_2$ magnetic solids.

The structures of these magnetic solids were inferred to be disordered, three-dimensional networks of V^{II} cations bridged by radical anion forms of the organic acceptors. XANES/EXAFS studies of the related V[TCNE]$_2$ ferrimagnet suggest that the V^{II} ion is surrounded by six nitrile nitrogen atoms in a pseudo-octahedral ligand field [21,22]. Theoretical studies indicate that the lowest-energy structure of V[TCNE]$_2$ includes two-dimensional layers of μ_4-$TCNE^{\bullet-}$ and V^{II} spanned by μ_2-$TCNE^{\bullet-}$ struts. [23] In the case of the presented solids, this structure is likely to be inaccessible due to the steric bulk of the chlorinated phenyl rings and the presence of only three CN groups that can bridge the V^{II} ions. The IR spectra of the neutral acceptors and the corresponding magnets exhibited characteristic C≡N stretching frequencies between 2100 and 2250 cm^{-1}. The shift to lower energies for the C≡N bands

of the magnets was consistent with the reduction of the nitrile bond order due to the presence of the radical anion located on the olefin. The IR data for the C≡N bands of the magnets and neutral acceptors are summarized in Table 1.

Table 1. Summary of CN stretching frequency data for neutral acceptors and resulting magnets.

Acceptor	Neutral Acceptor	Magnet
	ν_{CN}, cm^{-1}	ν_{CN}, cm^{-1}
H_5PTCE	2235, 2233	2210, 2129
2-ClPTCE	2241	2210, 2128
3-ClPTCE	2240	2208, 2130
4-ClPTCE	2237, 2230	2207, 2128
2,3-Cl_2PTCE	2243	2204, 2132
2,4-Cl_2PTCE	2241	2208, 2135
2,5-Cl_2PTCE	2242, 2228	2198, 2132
2,6-Cl_2PTCE	2244, 2229	2200, 2128
3,5-Cl_2PTCE	2238	2199, 2133
2,3,6-Cl_3PTCE	2244, 2226	2201, 2136
2,3,5,6-Cl_4PTCE	2247, 2238, 2225	2198, 2133

The measurement results of the magnetization versus applied field, M(H), are summarized in Table 2 and a representative plot of V[2,3,5,6-Cl4PTCE]$_2$ is shown in Figure 2. The coercivities of ~5 G observed here were smaller than those observed for V[TCNE]$_2$ (60 G) [1], but were consistent with the $S = {}^3/_2$, $(t_{2g})^3(e_g)^0$, $^4A_2$ ground state of V^{II} in a pseudo-octahedral or lower symmetry ligand field, which produces minimal single-ion magnetic anisotropy [24]. Magnetization reached saturation at 100 G, and the saturation magnetization values ranged from 4400 to 5000 emu·G/mol for these samples. The saturation values were far smaller than the ~28,000 emu·G/mol expected for ferromagnetic coupling and were much closer to the ideal value of 5585 emu·G/mol predicted (assuming $g = 2$) for $S = {}^3/_2$ V^{II} coupled antiferromagnetically to two $S = {}^1/_2$ x-Cl_nPTCE radical anions. The presence of a diamagnetic dimer formation may contribute to lower rather than ideal saturation magnetization, analogous to $[TCNE]_2^{2-}$ dimers found in model compounds and related antiferromagnets [25–27]. Taken together, the above data allow these magnetic network solids to be conclusively categorized as soft ferrimagnets.

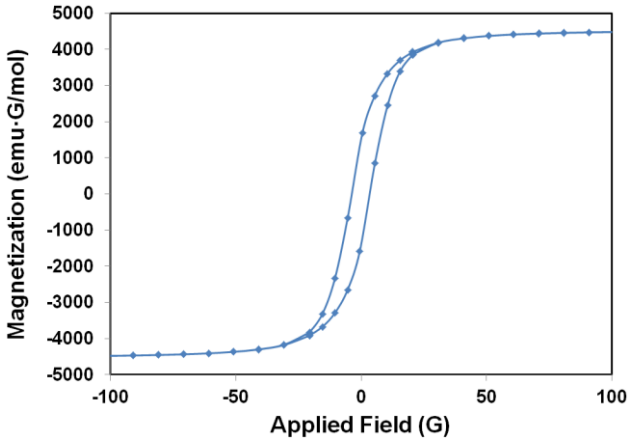

Figure 2. Magnetization hysteresis curve for V[2,3,5,6-Cl4PTCE]$_2$ collected at 5 K.

Field-cooled magnetization versus temperature data, M(T), were collected immediately after magnet synthesis (Figure 3), since previous studies have noted slight decreases in the T_c for aged samples [19]. The T_c for each sample was estimated by extrapolation to zero magnetization from the steepest portion of the M(T) curves. The reported T_c values were averaged from at least two preparations. Ranges for deviation in T_c (Table 2) were small (±2 K), demonstrating the reproducibility

of the T_c data. During the M(T) experiments, sample magnetizations decreased slowly from 5 K until ~30 K below T_c (Figure 3). The relatively sharp transition near T_c suggests some degree of magnetic and structural uniformity in these materials. The T_c of each magnet ranged from 146 K to 285 K depending on the position of the chlorine substitution.

Table 2. Summary of magnetic data and associated acceptor properties.

Acceptor	T_c (K)	Var. in T_c (K)	No. of Meas.	M_s ($\frac{emu \cdot G}{mol}$)	H_c ($\frac{emu \cdot G}{mol}$)	$E_{1/2}$ (V)	EA (eV)	Anion Dihedral (Degrees)
H_5PTCE *	213	±2	2	5100	2.0	−0.40	2.64	16.5
2-ClPTCE	271	±1	3	4700	3.1	−0.34	2.67	38.2
3-ClPTCE	243	±1	2	4900	4.8	−0.28	2.84	15.3
4-ClPTCE	146	±2	2	4400	6.8	−0.32	2.81	14.8
2,3-Cl_2PTCE	265	±2	3	4300	4.2	−0.29	2.80	38.3
2,4-Cl_2PTCE	256	±1	2	5000	3.9	−0.29	2.83	37.0
2,5-Cl_2PTCE	265	±1	3	4400	4.1	−0.26	2.85	38.1
2,6-Cl_2PTCE	285	±2	3	4900	4.1	−0.28	2.66	62.1
3,5-Cl_2PTCE	257	±2	2	4800	4.2	−0.20	3.02	14.6
2,3,6-Cl_3PTCE	276	±2	2	4600	2.6	−0.23	2.79	60.9
2,3,5,6-Cl_4PTCE	256	±1	3	4500	3.6	−0.20	2.89	61.0

* Previous work [19].

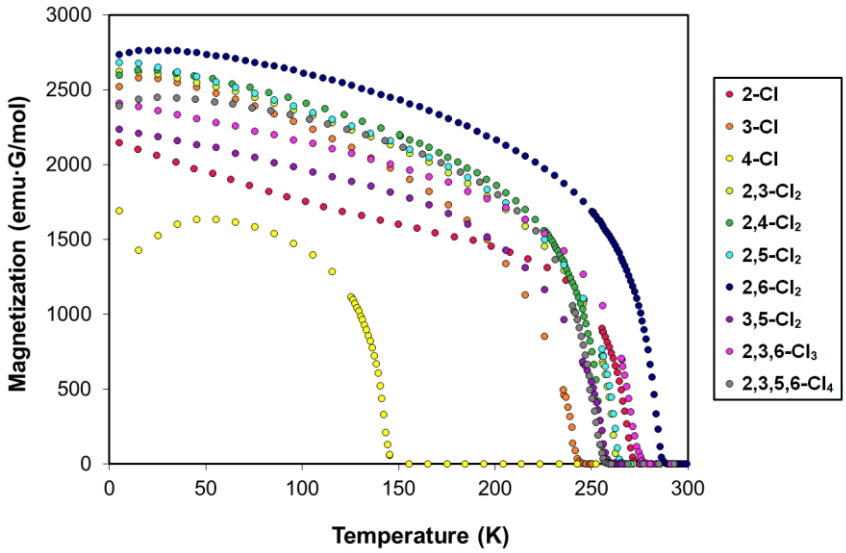

Figure 3. Variable-temperature magnetization data for V[x-Cl_nPTCE]$_2$ magnets. The legend indicates the substitution pattern of chlorine atoms in the organic unit.

3. Discussion

In order to facilitate discussion of the observed substituent effects, it is useful to consider the change in the T_c of each magnet relative to the unsubstituted V[H_5PTCE]$_2$ magnet. The T_c values for the chlorine substituted magnets are tabulated below, and the T_c data for the analogous fluorine substituted magnets reported previously are provided for reference (Table 3) [18,20]. Among the three monosubstituted acceptors, chlorine substitution appears to have a similar, albeit larger effect on T_c as fluorine substitution. Namely, substitutions in the 2-position result in magnets with large increases in T_c (V[2-ClPTCE]$_2$ T_c = 271 K, V[2-FPTCE]$_2$ T_c = 257 K) relative to the unsubstituted acceptor (V[H_5PTCE]$_2$ T_c = 213 K). Substitution at the 3-position results in a smaller, yet significant increase in T_c (V[3-ClPTCE]$_2$ T_c = 243 K, V[3-FPTCE]$_2$ T_c = 233 K). Substitution in the 4-position results in significant depression of T_c (V[4-ClPTCE]$_2$ T_c = 146 K, V[4-FPTCE]$_2$ T_c = 160 K).

Table 3. Comparison of T_c for the halogenated PTCE magnets (values for X = F taken from previous reports [18,20]).

Acceptor	X = Cl	X = F
	T_c (K)	T_c (K)
2-XPTCE	271	257
3-XPTCE	243	233
4-XPTCE	146	160
2,3-X_2PTCE	265	
2,4-X_2PTCE	256	242
2,5-X_2PTCE	265	
2,6-X_2PTCE	285	300
3,5-X_2PTCE	257	263
2,3,6-X_3PTCE	276	310
2,3,5,6-X_4PTCE	256	315

It was previously observed that the effect of multiple fluorine substitutions was to magnify the same changes observed for the monosubstituted samples. For instance, the 2-position enhancement and 4-position depression partially cancel out (V[2-FPTCE]$_2$ T_c = 257 K vs. V[2,4-F2PTCE]$_2$ T_c = 242 K vs. V[4-FPTCE]$_2$ T_c = 160 K), and the same effect was found here for chlorine substitution (V[2-ClPTCE]$_2$ T_c = 271 K vs. V[2,4-Cl2PTCE]$_2$ T_c = 256 K vs. V[4-ClPTCE]$_2$ T_c = 146 K). Similarly, multiple substitutions in the equivalent 2- and 6-positions magnified the T_c enhancement for both fluorine (V[2,6-F2PTCE]$_2$ T_c = 300 K vs. V[2-FPTCE]$_2$ T_c = 257 K) and chlorine (V[2,6-Cl2PTCE]$_2$ T_c = 285 K vs. V[2-ClPTCE]$_2$ T_c = 271 K) PTCE magnets, and multiple substitutions in the equivalent 3- and 5- positions magnified the T_c enhancement for both fluorine (V[3,5-F2PTCE]$_2$ T_c = 263 K vs. V[3-FPTCE]$_2$ T_c = 233 K) and chlorine (V[3,5-Cl2PTCE]$_2$ T_c = 257 K vs. V[3-ClPTCE]$_2$ T_c = 243 K) PTCE magnets. However, combining 2/6- and 3/5- substitutions revealed stark differences between chlorine and fluorine substitution. For fluorine substitution, the T_c was always enhanced by adding additional fluorine substituents to the four positions that enhance T_c (V[2,6-F2PTCE]$_2$ T_c = 300 K vs. V[2,3,6-F3PTCE]$_2$ T_c = 310 K vs. V[2,3,5,6-F4PTCE]$_2$ T_c = 315 K), whereas the 2/6- position chlorine substituted magnet was adversely affected by adding 3/5- position substituents (V[2-ClPTCE]$_2$ T_c = 271 K vs. V[2–3-Cl2PTCE]$_2$ T_c = 265 K vs. V[2,5-Cl2PTCE]$_2$ T_c = 265 K, and V[2,6-Cl2PTCE]$_2$ T_c = 285 K vs. V[2,3,6-Cl3PTCE]$_2$ T_c = 276 K vs. V[2,3,5,6-Cl4PTCE]$_2$ T_c = 256 K). In the following discussion, we aim to disentangle the various electronic and structural factors that chlorine substitution has on the observed trends in T_c for these PTCE magnets.

In order to discuss the electronic effects of chlorine substitution, it is useful to first build a simple molecular orbital model of the V^{II}-acceptor$^{\bullet-}$ bonding in these systems. Carlegrim et al. examined analogous V[TCNE]$_2$ systems by near-edge x-ray absorption fine structure and photoelectron spectroscopies [28]. Their results suggest that the π^* singly occupied molecular orbital (SOMO) of the TCNE$^{\bullet-}$ radical anion is very close in energy to the partially occupied t_{2g} orbitals (POMO) of V^{II} in a pseudo-octahedral ligand field, which facilitates strong covalent bonding and consequent strong ferrimagnetic communication (large magnetic exchange coupling). Ab initio DFT studies corroborate the placement of these energy levels for V[TCNE]$_2$ [23,29]. The parent H_5-PTCE ligand is a poorer electron acceptor ($E_{1/2}$ = −0.40 vs. Ag/AgCl) than TCNE ($E_{1/2}$ = +0.11 vs Ag/AgCl), thus the SOMO π^* orbitals for H_5-PTCE are assumed to lie higher in energy than the vanadium POMO t_{2g} orbitals (Figure 4). The increased energy gap between the metal and ligand valance orbitals weakens the covalent bonding interaction, and the consequently smaller magnetic exchange coupling results in a lower T_c for V[H_5-PTCE]$_2$ magnets relative to V[TCNE]$_2$ magnets. The addition of electron-withdrawing chlorine or fluorine substituents to the parent H_5PTCE would be expected to lower the π^* SOMO of the x-Cl_nPTCE acceptors, which should increase the V^{II}-Cl_nPTCE$^{/-}$ covalent bonding and thus lead to larger magnetic exchange coupling and a higher T_c.

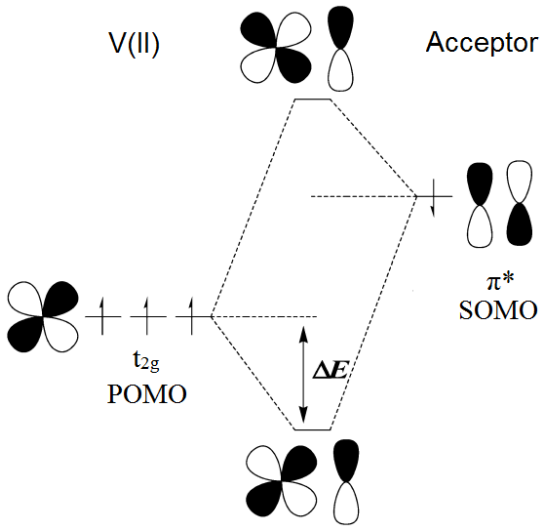

Figure 4. Molecular orbital schematic showing the relative energies of the valence orbitals on V^{II} and the x-Cl_nPTCE one-electron acceptors.

The predictions of our simple molecular orbital model were mostly borne out when we first limit the discussion to only those acceptors that have small calculated dihedral angles between the phenyl ring and the olefin, i.e., only those acceptors where electronics are expected to have the most important effect (H_5-PTCE, 3-ClPTCE, 3,5-Cl_2PTCE, and 4-ClPTCE). In particular, we noted the clear correlation (R = 0.991) between $E_{1/2}$ and T_c for H_5-PTCE, 3-ClPTCE, and 3,5-Cl_2PTCE, where each additional chlorine substitution made it easier to reduce the acceptor (owing to a lower-energy SOMO) and raised the observed T_c of the corresponding magnet (Figure 5). Substituting the calculated electron affinities for the measured redox potentials provided a similarly good correlation to the T_c data (R = 0.97, see SI).

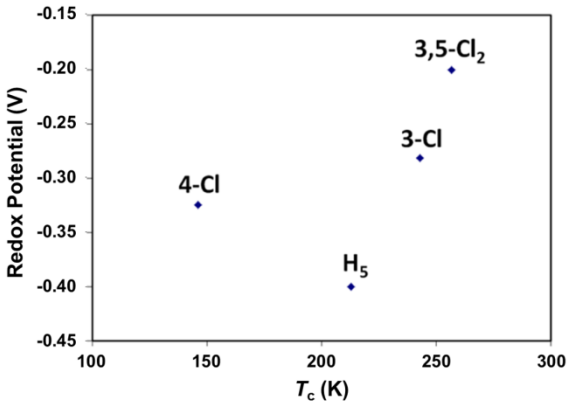

Figure 5. Redox potential (taken as the average of the cathodic and anodic peaks measured by cyclic voltammetry and denoted as $E_{1/2}$), vs. the ordering temperature (T_c) for planar V[x-Cl_nPTCE]$_2$ magnets.

However, the 4-ClPTCE magnet is clearly an unexplained outlier. The 4-ClPTCE acceptor was slightly harder to reduce than 3-ClPTCE because chlorine (like fluorine) is partly electron donating by resonance in the ortho/para positions (Hammett parameters σ_p are less than σ_m for both chlorine and fluorine) [30]. However, neither the reduction potential nor the Hammett parameters can explain why the T_c of 4-ClPTCE magnet was lower than that of the unsubstituted H_5-PTCE magnet. It is worth considering that aryl-chlorine (and aryl-fluorine) bonds can act as reasonable sites for oxidative addition, where a low valent metal attacks the aryl-halogen bond in a manner similar to nucleophilic aromatic substitution (NAS). Hence, we propose that the electron-rich V(0) may act as a nucleophile and bind to this site in the solid, generating magnetic coupling pathways that are deleterious to high T_c [31]. Several authors have shown that low valent metals can react with aryl-halogen bonds in the

presence of electron withdrawing groups, and it has been shown that halogen substituents that are para to an electron withdrawing group are particularly vulnerable [32–36]. It is also worth noting that the strongly electron donating 4-MePTCE has a T_c well above that of either 4-ClPTCE or 4-FPTCE, which lends support to the proposal that NAS may play a role in the 4-X halogen substituted magnets [37].

Rationalization of the trend in T_c for the remaining chlorine-substituted magnets requires consideration of the role of steric factors. The large size of chlorine substitution (relative to hydrogen) in the 2/6-positions causes a substantial increase in the dihedral angle between the phenyl ring and the olefin. The increased dihedral angle would be expected to attenuate the electronic conjugation between the phenyl ring and the olefin, which should reduce the electronic effects of any chlorine substitutions on the V^{II}-nitrile bonding interactions. The DFT-minimized gas-phase dihedral angles were found to be around 15° with no 2- or 6-position substitutions, while one 2-position substitution had a dihedral of ~38°, and substitution in both the 2- and 6- positions provided a dihedral of ~61° (Figure 6). The effect was similar, albeit reduced in magnitude for the fluorine substitutions, where substitution in both the 2- and 6-positions provided a dihedral of ~46°.

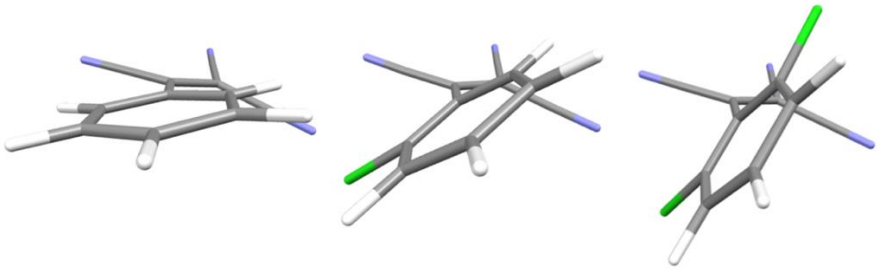

Figure 6. DFT-minimized structures of H_5-PTCE (**left**), 2-ClPTCE (**middle**), and 2,6-Cl_2PTCE (**right**) radical anions that show an increase in the dihedral angle as more chlorine substituents are added in the 2- and 6- positions.

The high T_c values of the magnets with 2- and/or 6-position chlorine substitutions can be qualitatively rationalized by considering the effect of reduced phenyl-olefin conjugation on these systems. As the dihedral angle is increased, a greater portion of the unpaired spin density is localized onto the nitrile nitrogen atoms. Consequently, the amount of spin density on the phenyl ring is reduced, which is supported by the DFT calculations (Supplementary Materials). Since the nitrile nitrogen atoms are directly involved in bonding to the V^{II} centers, it stands to reason that localization of increased spin density on those atoms would facilitate enhanced magnetic communication between the V^{II} and acceptor and lead to a higher T_c. The proposed correlation between T_c and nitrile spin density (Figure 7) is at least partially supported by the data. At a low dihedral angle, the magnetic ordering temperatures spanned a wide range, which is consistent with the significant electronic effects observed in that regime. At higher dihedral angles and nitrile nitrogen spin densities, the ordering temperatures are more tightly clustered, consistent with the loss of electronic conjugation between the olefin and the ring. It is worth noting that the 2,6-Cl_2PTCE magnet has both the highest T_c and highest nitrile spin density among this family of acceptors.

It remains an ongoing mystery as to why combining 2/6- and 3/5- substitutions results in a lower T_c for chlorine substituted magnets, but a higher T_c for fluorine substituted magnets. The larger dihedral angles of the 2/6- chlorine substituted acceptors would be expected to attenuate the beneficial effects of 3/5- substitution, but the reversal of the trend relative to fluorine substitutions is difficult to explain. Nonetheless, the T_c data for the 2,3-Cl_2, 2,5-Cl_2, 2,3,6-Cl_3, and 2,3,5,6-Cl_4 magnets all support that unexpected reversal of the trend. Other factors not considered by our current model must also play a significant role, although these effects are likely to be steric in nature given the electronic similarities of chlorine and fluorine substitution. For example, increased steric bulk for the 3/5-substitutions (or anywhere on the phenyl ring) may negatively impact the ability to form V^{II} -PTCE$^{\bullet-}$ contacts, and

the consequently lower average molecular weight V^{II}-$PTCE^{\bullet-}$ networks would be expected to have a lower T_c.

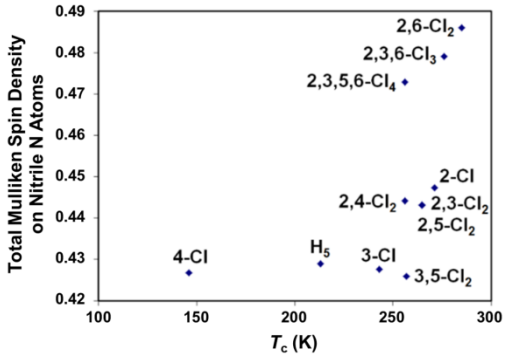

Figure 7. Mulliken spin density vs. T_c for the chlorine-substituted PTCE magnets.

4. Materials and Methods

General Considerations: Preparations of the air-sensitive magnetic samples were carried out in a nitrogen-filled Vacuum Atmospheres glovebox. Vanadium hexacarbonyl and its precursor salt, $[Et_4N][V(CO)_6]$, were prepared according to procedure described in the literature [38]. Anhydrous dimethylformamide, n-butyllithium, N-chlorosuccinimide, 1,2,4,5-tetrachlorobenzene, 1-bromo-3,5-dichlorobenzene, and the chlorine substituted benzaldehydes were purchased from Alfa Aesar. Malononitrile, piperidine, and 1,2,4-trichlorobenzene were purchased from Aldrich. Magnesium turnings were purchased from Fischer and potassium cyanide was purchased from Acros. All reagents were used as received except as noted below. Dichloromethane was distilled from P_2O_5, followed by distillation from CaH_2 under argon prior to use in the synthesis of the magnetic samples. Tetrahydrofuran was refluxed over sodium benzophenone ketyl and distilled under argon prior to use. All chlorinated acceptors were synthesized based on a modified literature procedure described below [39]. Flash chromatography was performed using Silicycle SiliaFlash P60 silica (230–400 mesh). Purity of the chlorophenyltricyanoethylenes was confirmed by sharp melting transitions and by ^1H NMR spectroscopy. In all cases, acceptor purity was estimated to be greater than 99%. Melting points were uncorrected. NMR spectra were obtained using a JEOL EclipsePlus-500 spectrometer operating at 500 MHz for ^1H and 125 MHz for ^{13}C. Chemical shifts for ^1H (or ^{13}C) were reported in parts per million relative to the solvent resonance, taken as δ 7.26 (δ 77.16) for $CDCl_3$. Elemental analyses were performed by Galbraith Laboratories, Knoxville, TN, USA.

Magnetic Measurements: Magnetic measurements were performed on a 7 T Quantum Design MPMS SQUID magnetometer. Powder samples were packed in glass tubes, and sealed under vacuum as previously described [40]. M vs. T experiments were performed by cooling to 5 K in a 100 G applied field and measured in a 5 G applied field upon warming from 5 to 300 K. Measurements of magnetization as a function of the applied magnetic field were performed at 5 K. Diamagnetic corrections were not applied to the magnetic data.

Electrochemistry Measurements: Cyclic voltammograms were recorded using a CH Instruments model 600A potentiostat. Measurements were performed on ~5 mM solutions in freshly distilled and degassed CH_3CN with 0.1 M $[n\text{-}Bu_4N][PF_6]$ as the supporting electrolyte. Data were collected between −1.2 V and 0.5 V at a scan rate of 0.1 V/s using a polished platinum working electrode, a platinum wire auxiliary electrode, and an aqueous Ag/AgCl reference electrode. Solution resistance was compensated 90% using positive-feedback IR compensation for all measurements. Redox potentials ($E_{1/2}$) were reported as the average of the anodic and cathodic peaks relative to the Ag/AgCl reference. In order to facilitate comparison to previously published data where a glassy carbon working electrode was used instead of polished platinum, the measured redox potentials were adjusted so that the ferrocene

internal standard was set to 0.45 V, which is the known potential of ferrocene vs. Ag/AgCl using a glassy carbon working electrode [41].

Density Functional Theory Calculations. Geometry optimization calculations were performed using the B3LYP density functional and 6-311++G(d,p) basis set within Gaussian09 [42]. Minimized structures for both the neutral and anionic forms of each chlorinated acceptor were calculated, and these coordinates are tabulated in the Supplementary Materials). Electron affinities (E_{ea}) of the neutral acceptors were calculated by subtracting the zero-point energy self-consistent field energy values of the radical anion from the corresponding neutral acceptor. This method has been shown to provide estimations of E_{ea} for a number of organic molecules with good comparison to the experimental data [43].

General procedure for the synthesis of the organic one-electron acceptors: The general procedure outlined in Scheme 1 has been described previously, and a representative example can be found in the Supplementary Materials [18–20].

Synthesis of 2-(2-chlorophenyl)-1,1,2-tricyanoethylene (2-ClPTCE). Yield: 43% over three steps. Mp: 127.5–127.9 °C. IR (KBr): ν_{CN} 2241 cm^{-1}. ^{1}H NMR δ 7.51 (m, 2H), 7.62 (m, 2H). ^{13}C NMR δ 100.86, 109.63, 110.04, 112.39, 127.46, 128.26, 130.74, 131.53, 133.34, 134.97, 141.07. HRMS-FAB (m/z, $[M + 2H]^+$) Calcd for $C_{11}H_6ClN_3$: 215.02502, Found: 215.02474.

Synthesis of 2-(3-chlorophenyl)-1,1,2-tricyanoethylene (3-ClPTCE). Yield: 42% over three steps. Mp: 72.8–73.4 °C. IR (KBr): ν_{CN} 2240 cm^{-1}. ^{1}H NMR δ 7.59 (t, J = 8.0 Hz, 1H), 7.70 (m, 1H), 7.90 (m, 1H), 7.94 (t, J = 2.0 Hz, 1H). ^{13}C NMR δ 94.61, 110.66, 110.90, 113.43, 127.54, 129.40, 129.91, 131.45, 135.62, 136.62, 140.61. HRMS-FAB (m/z, $[M]^+$) Calcd for $C_{11}H_4ClN_3$: 213.00937, Found: 213.01012.

Synthesis of 2-(4-chlorophenyl)-1,1,2-tricyanoethylene (4-ClPTCE). Yield: 21% over three steps. Mp: 172.4–172.9 °C. IR (KBr): ν_{CN} 2237 and 2230 cm^{-1}. ^{1}H NMR δ 7.61 (m, 2H), 7.97 (m, 2H). ^{13}C NMR δ 93.08, 111.02, 111.15, 113.54, 126.91, 130.68, 130.93, 140.68, 142.93. HRMS-FAB (m/z, $[M]^+$) Calcd for $C_{11}H_4ClN_3$: 213.00937, Found: 213.00966.

Synthesis of 2-(2,3-dichlorophenyl)-1,1,2-tricyanoethylene (2,3-Cl_2PTCE). Yield: 54% over three steps. Mp: 137.2–137.7 °C. IR (KBr): ν_{CN} 2243 cm^{-1}. ^{1}H NMR δ 7.41 (dd, ^{3}J = 7.8 Hz, ^{4}J = 1.6 Hz, 1H), 7.47 (t, J = 7.9 Hz, 1H), 7.77 (dd, ^{3}J = 8.0 Hz, ^{4}J = 1.6 Hz, 1H). ^{13}C NMR δ 101.53, 109.33, 109.78, 112.07, 128.79, 128.89, 129.18, 131.66, 135.38, 135.90, 140.38. HRMS-FAB (m/z, $[M]^+$) Calcd for $C_{11}H_3Cl_2N_3$: 246.97040, Found: 246.97069.

Synthesis of 2-(2,4-dichlorophenyl)-1,1,2-tricyanoethylene (2,4-Cl_2PTCE). Yield: 42% over three steps. Mp: 102.8–103.5 °C. IR (KBr): ν_{CN} 2241 cm^{-1}. ^{1}H NMR δ 7.47 (d, J = 8.4 Hz, 1H), 7.50 (dd, ^{3}J = 8.5 Hz, ^{4}J = 1.9 Hz, 1H), 7.65 (d, J = 1.9 Hz, 1H). ^{13}C NMR δ 101.12, 109.53, 109.89, 112.14, 125.78, 128.84, 131.53, 131.65, 134.37, 139.90, 141.31. HRMS-FAB (m/z, $[M + 2H]^+$) Calcd for $C_{11}H_5Cl_2N_3$: 248.98605, Found: 248.98621.

Synthesis of 2-(2,5-dichlorophenyl)-1,1,2-tricyanoethylene (2,5-Cl_2PTCE). Yield: 45% over three steps. Mp: 111.0–111.5 °C. IR (KBr): ν_{CN} 2242 and 2228 cm^{-1}. ^{1}H NMR δ 7.49 (dd, ^{4}J = 2.2 Hz, ^{5}J = 0.6 Hz, 1H), 7.56 (dd, ^{3}J = 8.7 Hz, ^{5}J = 0.5 Hz, 1H), 7.59 (dd, ^{3}J = 8.7 Hz, ^{4}J = 2.2 Hz, 1H). ^{13}C NMR δ 101.94, 109.27, 109.71, 112.06, 128.46, 130.22, 131.55, 132.66, 134.55, 134.83, 139.41. HRMS-FAB (m/z, $[M + 2H]^+$) Calcd for $C_{11}H_5Cl_2N_3$: 248.98605, Found: 248.98653.

Synthesis of 2-(2,6-dichlorophenyl)-1,1,2-tricyanoethylene (2,6-Cl_2PTCE). Yield: 33% over three steps. Mp: 122.1–122.8 °C. IR (KBr): ν_{CN} 2244 and 2229 cm^{-1}. ^{1}H NMR δ 7.54 (s, 3H). ^{13}C NMR δ 104.39, 108.89, 109.41, 111.63, 126.21, 129.41, 134.30, 134.41, 138.44. HRMS-FAB (m/z, $[M + H]^+$) Calcd for $C_{11}H_4Cl_2N_3$: 247.97823, Found: 247.97889.

Synthesis of 2-(3,5-dichlorophenyl)-1,1,2-tricyanoethylene (3,5-Cl_2PTCE). Yield: 35% over three steps. Mp: 142.3–143.3 °C. IR (KBr): ν_{CN} 2238 cm^{-1}. ^{1}H NMR δ 7.71 (t, ^{4}J = 1.8 Hz, 1H), 7.83 (d, ^{4}J = 1.8 Hz, 2H).

^{13}C NMR δ 96.08, 110.22, 110.54, 113.11, 127.48, 130.68, 135.18, 137.39, 139.27. HRMS-FAB (m/z, [M + 2H]$^+$) Calcd for $C_{11}H_5Cl_2N_3$: 248.98605, Found: 248.98652.

Synthesis of 2-(2,3,6-trichlorophenyl)-1,1,2-tricyanoethylene (2,3,6-Cl_3PTCE). Yield: 38% over three steps. Mp: 135.1–135.8 °C. IR (KBr): ν_{CN} 2244 and 2226 cm^{-1}. ^{1}H NMR δ 7.50 (d, ^{3}J = 8.8 Hz, 1H), 7.69 (d, ^{3}J = 8.8 Hz, 1H). ^{13}C NMR δ 104.63, 108.68, 109.22, 111.37, 127.57, 129.92, 132.28, 132.73, 133.94, 134.85, 137.81. HRMS-FAB (m/z, [M + H]$^+$) Calcd for $C_{11}H_3Cl_3N_3$: 281.93926, Found: 281.94001.

Synthesis of 2-(2,3,5,6-tetrachlorophenyl)-1,1,2-tricyanoethylene (2,3,5,6-Cl_4PTCE). Yield: 51% over three steps. Mp: 150.1–151.2 °C. IR (KBr): ν_{CN} 2247, 2238 and 2225 cm^{-1}. ^{1}H NMR δ 7.88 (s, 1H). ^{13}C NMR δ 104.80, 108.50, 109.05, 111.13, 128.52, 130.97, 134.16, 134.85, 137.36. HRMS-FAB (m/z, [M]$^+$) Calcd for $C_{11}H_1Cl_4N_3$: 314.89246, Found: 314.89288.

General procedure for the synthesis of V[Cl_xPTCE]$_2$·yCH_2Cl_2 Magnets: Under a nitrogen atmosphere, vanadium hexacarbonyl (15.3 mg, 0.070 mmol) dissolved in dichloromethane (2 mL) was added quickly to a solution containing Cl_xPTCE (0.15 mmol) in dichloromethane (1 mL) with stirring. After 15 min, the black precipitate was collected on a medium porosity frit, rinsed with dichloromethane (2 × 2 mL), and dried in vacuo for 1 h to yield a black powder of the desired product.

Synthesis of V[2-ClPTCE]$_2$. Yield: 32.5 mg (98%). IR (KBr): ν_{CN} 2210 and 2128 cm^{-1}. Anal. Calcd (Found) $C_{22}H_8Cl_2N_6V_1$: C 55.26 (55.29), H 1.69 (2.32), N 17.57 (17.35) %.

Synthesis of V[3-ClPTCE]$_2$·0.05CH_2Cl_2. Yield: 33.5 mg (99%). IR (KBr): ν_{CN} 2208 and 2130 cm^{-1}. Anal. Calcd (Found) $C_{22}H_8Cl_2N_6V_1$·0.05CH_2Cl_2: C 54.90 (54.88), H 1.69 (1.85), N 17.42 (17.52) %.

Synthesis of V[4-ClPTCE]$_2$·0.35CH_2Cl_2. Yield: 32.3 mg (91%). IR (KBr): ν_{CN} 2207 and 2128 cm^{-1}. Anal. Calcd (Found) $C_{22}H_8Cl_2N_6V_1$·0.35CH_2Cl_2: C 52.85 (52.82), H 1.73 (1.79), N 16.55 (16.76) %.

Synthesis of V[2,3-Cl2PTCE]$_2$·0.05CH_2Cl_2. Yield: 32.3 mg (84%).IR (KBr): ν_{CN} 2204 and 2132 cm^{-1}. Anal. Calcd (Found) $C_{22}H_6Cl_4N_6V_1$·0.05CH_2Cl_2: C 48.04 (48.04), H 1.12 (1.14), N 15.24 (15.03) %.

Synthesis of V[2,4-Cl2PTCE]$_2$·0.10CH_2Cl_2. Yield: 33.4 mg (86%). IR (KBr): ν_{CN} 2208 and 2135 cm^{-1}. Anal. Calcd (Found) $C_{22}H_6Cl_4N_6V_1$·0.10CH_2Cl_2: C 47.78 (48.15), H 1.12 (1.57), N 15.13 (15.28) %.

Synthesis of V[2,5-Cl2PTCE]$_2$·0.30CH_2Cl_2. Yield: 38.7 mg (97%). IR (KBr): ν_{CN} 2198 and 2132 cm^{-1}. Anal. Calcd (Found) $C_{22}H_6Cl_4N_6V_1$·0.30CH_2Cl_2: C 46.78 (46.71), H 1.16 (1.29), N 14.68 (14.97) %.

Synthesis of V[2,6-Cl2PTCE]$_2$·0.50CH_2Cl_2. Yield: 35.5 mg (86%). IR (KBr): ν_{CN} 2200 and 2128 cm^{-1}. Anal. Calcd (Found) $C_{22}H_6Cl_4N_6V_1$·0.50CH_2Cl_2: C 45.84 (45.82), H 1.20 (1.53), N 14.25 (14.50) %.

Synthesis of V[3,5-Cl2PTCE]$_2$·0.30CH_2Cl_2. Yield: 37.3 mg (93%). IR (KBr): ν_{CN} 2199 and 2133 cm^{-1}. Anal. Calcd (Found) $C_{22}H_6Cl_4N_6V_1$·0.30CH_2Cl_2: C 46.78 (46.64), H 1.16 (1.29), N 14.68 (14.82) %.

Synthesis of V[2,3,6-Cl3PTCE]$_2$·0.45CH_2Cl_2. Yield: 42.2 mg (92%). IR (KBr): ν_{CN} 2201 and 2136 cm^{-1}. Anal. Calcd (Found) $C_{22}H_4Cl_6N_6V_1$·0.45CH_2Cl_2: C 41.05 (41.05), H 0.77 (0.78), N 12.77 (13.17) %.

Synthesis of V[2,3,5,6-Cl4PTCE]$_2$·0.20CH_2Cl_2. Yield: 48.6 mg (99%). IR (KBr): ν_{CN} 2198 and 2133 cm^{-1}. Anal. Calcd (Found) $C_{22}H_2Cl_8N_6V_1$·0.20CH_2Cl_2: C 37.99 (37.99), H 0.34 (<0.5), N 11.97 (12.03) %.

5. Conclusions

The foregoing results demonstrate that chlorine-substituted phenyltricyanoethylenes can be building blocks for the formation of magnetically ordered solids with T_cs from 146 to 285 K. Importantly, this work expands the list of organic one-electron acceptors that can react with $V(CO)_6$ to form high T_c magnets. No single property of the acceptors yielded a satisfactory correlation with T_c, although smaller subsets of the data could be successfully rationalized according to electronic and steric effects. In general, chlorine substitutions were inductively electron withdrawing, making the corresponding acceptors easier to reduce, and the corresponding magnets had enhanced T_c relative to the unsubstituted

H_5PTCE parent. Substitution in the 2- and/or 6-position(s) caused a large increase in the dihedral angle between the phenyl ring and olefin, which localized spin onto the nitrile nitrogen atoms and produced a material with a higher T_c. The anomalously low T_c of 4-FPTCE previously reported was reproduced by the anomalously low T_c of 4-ClPTCE, for which we have proposed a few explanations including a potentially deleterious reaction.

Supplementary Materials: The following are available online at http://www.mdpi.com/2312-7481/5/3/44/s1: ^{1}H and ^{13}C NMR spectra of all organic acceptors, tests of T_c versus redox potential, radical, and radical anion dihedral angle, and additional computational details.

Author Contributions: The authors have contributed equally to the conceptualization and execution of this work and wrote the manuscript together.

Funding: This research was partially funded by the National Science Foundation (grant number 0518220) and the Virginia Tech ASPIRES program (partial funding for the purchase of the SQUID magnetometer).

Conflicts of Interest: The authors declare no conflicts of interest.

References

1. Manriquez, J.M.; Yee, G.T.; Mclean, R.S.; Epstein, A.J.; Miller, J.S. A Room-Temperature Molecular/Organic-Based Magnet. *Science* **1991**, *252*, 1415–1417. [CrossRef] [PubMed]
2. Miller, J.S. Oliver Kahn Lecture: Composition and structure of the V[TCNE]$_x$ (TCNE = tetracyanoethylene) room-temperature, organic-based magnet—A personal perspective. *Polyhedron* **2009**, *28*, 1596–1605. [CrossRef]
3. Miller, J.S. Magnetically ordered molecule-based materials. *Chem. Soc. Rev.* **2011**, *40*, 3266–3296. [CrossRef] [PubMed]
4. Wegner, D.; Yamachika, R.; Zhang, X.; Wang, Y.; Baruah, T.; Pederson, M.R.; Bartlett, B.M.; Long, J.R.; Crommie, M.F. Tuning Molecule-Mediated Spin Coupling in Bottom-Up-Fabricated Vanadium-Tetracyanoethylene Nanostructures. *Phys. Rev. Lett.* **2009**, *103*, 087205. [CrossRef] [PubMed]
5. Yoo, J.-W.; Chen, C.-Y.; Jang, H.W.; Bark, C.W.; Prigodin, V.N.; Eom, C.B.; Epstein, A.J. Spin injection/detection using an organic-based magnetic semiconductor. *Nat. Mater.* **2010**, *9*, 638–642. [CrossRef] [PubMed]
6. Yu, H.; Harberts, M.; Adur, R.; Lu, Y.; Hammel, P.C.; Johnston-Halperin, E.; Epstein, A.J. Ultra-narrow ferromagnetic resonance in organic-based thin films grown via low temperature chemical vapor deposition. *Appl. Phys. Lett.* **2014**, *105*, 012407. [CrossRef]
7. Zhang, J.; Ensling, J.; Ksenofontov, V.; Gütlich, P.; Epstein, A.J.; Miller, J.S. [M^{II}(TCNE)$_2$] xCH_2Cl_2 (M = Mn, Fe, Co, Ni) Molecule-Based Magnets with T_c Values above 100 K and Coercive Fields up to 6500 Oe. *Angew. Chem. Int. Ed.* **1998**, *37*, 657–660. [CrossRef]
8. Pokhodnya, K.I.; Vickers, E.B.; Bonner, M.; Epstein, A.J.; Miller, J.S. Solid Solution V_xFe_{1-x}[TCNE]$_2$·zCH_2Cl_2 Room-Temperature Magnets. *Chem. Mater.* **2004**, *16*, 3218–3223. [CrossRef]
9. Vickers, E.B.; Senesi, A.; Miller, J.S. Ni[TCNE]$_2$ zCH_2Cl_2 (T_c = 13 K) and V_xNi_{1-x}[TCNE]$_y$ zCH_2Cl_2 solid solution room temperature magnets. *Inorg. Chim. Acta* **2004**, *357*, 3889–3894. [CrossRef]
10. Vickers, E.B.; Selby, T.D.; Thorum, M.S.; Taliaferro, M.L.; Miller, J.S. Vanadium 7,7,8,8-Tetracyano-*p*-quinodimethane (V[TCNQ]$_2$)-Based Magnets. *Inorg. Chem.* **2004**, *43*, 6414–6420. [CrossRef]
11. Vickers, E.B.; Selby, T.D.; Miller, J.S. Magnetically Ordered (T_c = 200 K) Bis(tetracyanopyrazine)vanadium, V[TCNP]$_2$·yCH_2Cl_2. *J. Am. Chem. Soc.* **2004**, *126*, 3716–3717. [CrossRef] [PubMed]
12. Taliaferro, M.L.; Thorum, M.S.; Miller, J.S. Room-Temperature Organic-Based Magnet ($T_c \approx 50$ °C) Containing Tetracyanobenzene and Hexacarbonylvanadate(−I). *Angew. Chem. Int. Ed.* **2006**, *118*, 5452–5457. [CrossRef]
13. Vickers, E.B.; Giles, I.D.; Miller, J.S. M[TCNQ]$_y$-Based Magnets (M = Mn, Fe, Co, Ni; TCNQ = 7,7,8,8-tetracyano-*p*-quinodimethane). *Chem. Mater.* **2005**, *17*, 1667–1672. [CrossRef]
14. Hao, J.; Davidson, R.A.; Kavand, M.; Schooten, K.J.; Schooten, K.J.; van Schooten, K.J.; Boehme, C.; Miller, J.S. Hexacyanobutadienide-Based Frustrated and Weak Ferrimagnets: M(HCBD)$_2$·zCH_2Cl_2 (M = V, Fe). *Inorg. Chem.* **2016**, *55*, 9393–9399. [CrossRef] [PubMed]
15. Pokhodnya, K.I.; Epstein, A.J.; Miller, J.S. Thin-Film V[TCNE]$_x$ Magnets. *Adv. Mater.* **2000**, *12*, 410–413. [CrossRef]

16. Lu, Y.; Yu, H.; Harberts, M.; Epstein, A.J.; Johnston-Halperin, E. Vanadium[ethyl tricyanoethylene carboxylate]x: A new organic-based magnet. *J. Mater. Chem. C* **2015**, *3*, 7363–7369. [CrossRef]
17. Fitzgerald, J.P.; Kaul, B.B.; Yee, G.T. Vanadium [dicyanoperfluorostilbene]$_2$·yTHF: A molecule-based magnet with $T_c \approx 205$ K. *Chem. Commun.* **2000**, 49–50. [CrossRef]
18. Harvey, M.D.; Crawford, T.D.; Yee, G.T. Room-Temperature and Near-Room-Temperature Molecule-Based Magnets. *Inorg. Chem.* **2008**, *47*, 5649–5655. [CrossRef] [PubMed]
19. Harvey, M.D.; Pace, J.T.; Yee, G.T. A room temperature ferrimagnet, vanadium [pentafluorophenyltricyanoethylene]$_2$. *Polyhedron* **2007**, *26*, 2037–2041. [CrossRef]
20. Amshumali, M.K.; Harvey, M.D.; Yee, G.T. Room temperature and near-room temperature coordination polymer magnets. *Synth. Met.* **2014**, *188*, 53–56. [CrossRef]
21. Haskel, D.; Islam, Z.; Lang, J.; Kmety, C.; Srajer, G.; Pokhodnya, K.I.; Epstein, A.J.; Miller, J.S. Local structural order in the disordered vanadium tetracyanoethylene room-temperature molecule-based magnet. *Phys. Rev. B* **2004**, *70*, 054422. [CrossRef]
22. Kortright, J.B.; Lincoln, D.M.; Edelstein, R.S.; Epstein, A.J. Bonding, Backbonding, and Spin-Polarized Molecular Orbitals: Basis for Magnetism and Semiconducting Transport in V[TCNE]$_2$. *Phys. Rev. Lett.* **2008**, *100*, 257204. [CrossRef] [PubMed]
23. Frecus, B.; Oprea, C.I.; Panait, P.; Ferbinteanu, M.; Cimpoesu, F.; Gîrţu, M.A. Ab initio study of exchange coupling for the consistent understanding of the magnetic ordering at room temperature in V[TCNE]$_x$. *Theor. Chem. Acc.* **2014**, *133*, 1470. [CrossRef]
24. Kahn, O. *Molecular Magnetism*; VCH: New York, NY, USA, 1993; ISBN 978-1-56081-566-2.
25. Novoa, J.N.; Ribas-Ariño, J.; Shum, W.W.; Miller, J.S. Control of Two-Electron Four-Center (2e-/4c) C−C Bond Formation Observed for Tetracyanoethenide Dimerization, $[TCNE]_2^{2-}$. *Inorg. Chem.* **2007**, *46*, 103–107. [CrossRef] [PubMed]
26. Wang, G.; Zhu, H.; Fan, J.; Slebodnick, C.; Yee, G.T. Coordination Complexes with cis-TCNE Radical Anion Ligands. Models of M[TCNE]$_2$ Magnets. *Inorg. Chem.* **2006**, *45*, 1406–1408. [CrossRef] [PubMed]
27. McConnell, A.C.; Shurdha, E.; Bell, J.D.; Miller, J.S. Antiferromagnetic Ordering of M^{II}(TCNE)[$C_4(CN)_8$]$_{1/2}$ (M = Mn, Fe; TCNE = Tetracyanoethylene). *J. Phys. Chem. C* **2012**, *116*, 18952–18957. [CrossRef]
28. Carlegrim, E.; Kanciurzewska, A.; de Jong, M.P.; Tengstedt, C.; Fahlman, M. The unoccupied electronic structure of the semi-conducting room temperature molecular magnet V(TCNE)$_2$. *Chem. Phys. Lett.* **2008**, *452*, 173–177. [CrossRef]
29. Erdin, S. Ab initio studies of tetracyanoethylene-based organic magnets. *Phys. B Condens. Matter* **2008**, *403*, 1964–1970. [CrossRef]
30. Hansch, C.; Leo, A.; Taft, R.W. A survey of Hammett substituent constants and resonance and field parameters. *Chem. Rev.* **1991**, *91*, 165–195. [CrossRef]
31. Goldstein, S.W.; Bill, A.; Dhuguru, J.; Ghoneim, O. Nucleophilic Aromatic Substitution—Addition and Identification of an Amine. *J. Chem. Educ.* **2017**, *94*, 1388–1390. [CrossRef]
32. Laev, S.S.; Shteingarts, V.D. Reductive dehalogenation of polyfluoroarenes by zinc in aqueous ammonia. *J. Fluor. Chem.* **1999**, *96*, 175–185. [CrossRef]
33. Lv, H.; Cai, Y.-B.; Zhang, J.-L. Copper-Catalyzed Hydrodefluorination of Fluoroarenes by Copper Hydride Intermediates. *Angew. Chem. Int. Ed.* **2013**, *52*, 3203–3207. [CrossRef] [PubMed]
34. Li, J.; Zheng, T.; Sun, H.; Li, X. Selectively catalytic hydrodefluorination of perfluoroarenes by Co(PMe_3)$_4$ with sodium formate as reducing agent and mechanism study. *Dalton Trans.* **2013**, *42*, 13048–13053. [CrossRef] [PubMed]
35. Reade, S.P.; Mahon, M.F.; Whittlesey, M.K. Catalytic Hydrodefluorination of Aromatic Fluorocarbons by Ruthenium *N*-Heterocyclic Carbene Complexes. *J. Am. Chem. Soc.* **2009**, *131*, 1847–1861. [CrossRef] [PubMed]
36. Schwartsburd, L.; Mahon, M.F.; Poulten, R.C.; Warren, M.R.; Whittlesey, M.K. Mechanistic Studies of the Rhodium NHC Catalyzed Hydrodefluorination of Polyfluorotoluenes. *Organometallics* **2014**, *33*, 6165–6170. [CrossRef]
37. King, J.A. Synthesis and Characterization of Molecule-Based Magnets Containing Methyl-Substituted Phenyltricyanoethylene Acceptors. Master's Thesis, Virginia Tech, Blacksburg, VA, USA, 2009.

38. Liu, X.; Ellis, J.E.; Mesaros, E.F.; Pearson, A.J.; Schoffers, E.; Hall, J.M.; Hoyne, J.H.; Shapley, J.R.; Fauré, M.; Saccavini, C.; et al. Transition Metal Carbonyl Compounds. In *Inorganic Syntheses*; Shapley, J.R., Ed.; John Wiley & Sons, Inc.: Hoboken, NJ, USA, 2004; pp. 93–132. ISBN 978-0-471-65368-4.
39. Corson, B.B.; Stoughton, R.W. Reactions of alpha, beta-unsaturated dinitriles. *J. Am. Chem. Soc.* **1928**, *50*, 2825–2837. [CrossRef]
40. Sellers, S.P.; Korte, B.J.; Fitzgerald, J.P.; Reiff, W.M.; Yee, G.T. Canted Ferromagnetism and Other Magnetic Phenomena in Square-Planar, Neutral Manganese(II) and Iron(II) Octaethyltetraazaporphyrins. *J. Am. Chem. Soc.* **1998**, *120*, 4662–4670. [CrossRef]
41. Thomas, K.R.J.; Tharmaraj, P.; Chandrasekhar, V.; Bryan, C.D.; Cordes, A.W. Synthesis, Spectroscopy, and Electrochemistry of Ternary Copper(II) Complexes with 2,2-Diphenyl-4,4,6,6-tetrakis(3,5-dimethylpyrazolyl)cyclotriphosphazene and Nitrogenous Bases. X-ray Structures of $N_3P_3Ph_2(3,5\text{-}Me_2Pz)_4{\cdot}Cu(ClO_4)_2{\cdot}2H_2O$ and $N_3P_3Ph_2(3,5\text{-}Me_2Pz)_4{\cdot}Cu(ClO_4)_2{\cdot}2ImH$. *Inorg. Chem.* **1994**, *33*, 5382–5390.
42. Frisch, M.J.; Trucks, G.W.; Schlegel, H.B.; Scuseria, G.E.; Robb, M.A.; Cheeseman, J.R.; Scalmani, G.; Barone, V.; Mennucci, B.; Petersson, G.A.; et al. *Gaussian 09, Revision D.01*; Gaussian Inc.: Wallingford, CT, USA, 2009.
43. Rienstra-Kiracofe, J.C.; Tschumper, G.S.; Schaefer, H.F.; Nandi, S.; Ellison, G.B. Atomic and Molecular Electron Affinities: Photoelectron Experiments and Theoretical Computations. *Chem. Rev.* **2002**, *102*, 231–282. [CrossRef]